DATE ISSUED DEC 22 1980

ORNL
MASTER COPY

OAK RIDGE NATIONAL LABORATORY
OPERATED BY
UNION CARBIDE CORPORATION
NUCLEAR DIVISION

POST OFFICE BOX X
OAK RIDGE, TENNESSEE 37830

SPECIAL DISTRIBUTION

ORNL
CENTRAL FILES NUMBER
ORNL/CF-80/354

8012 12

DATE: December 11, 1980

SUBJECT: Technical Highlights of Space and Terrestrial Systems Programs at Oak Ridge National Laboratory for August 1980

TO: Distribution

FROM: R. H. Cooper

This monthly report is intended to inform the Space and Terrestrial Systems Division, DOE, and their contractors of significant technical highlights of technology and systems support programs in progress at Oak Ridge National Laboratory. A detailed technical presentation of information will be published in topical reports and open literature publications.

NOTICE This document contains information of a preliminary nature and was prepared primarily for internal use at the Oak Ridge National Laboratory. It is subject to revision or correction and therefore does not represent a final report. The information is only for official use and no release to the public shall be made without the approval of the Law Department of Union Carbide Corporation, Nuclear Division.

SOLAR-POLAR MISSION MATERIALS SUPPORT 1

CBCF-3 Insulation Fabrication 1
CBCF-3 Characterization 2

FLIGHT SYSTEMS HARDWARE 7

Iridium Blank Fabrication 7
Meetings 8
Creep Properties of 2219 Aluminum Housing Materials 8

MATERIALS TECHNOLOGY SUPPORT 9

Impact Properties of M-Batch DOP-26 Alloy 9
Sulfur Embrittlement of DOP-26 Alloy 9
Effect of Phosphorus Contamination on Impact Properties of DOP-26 Alloy 9
AES Analysis of M-Lot DOP-26 Alloy 12
Development of Pt-Base Alloys 12

ISOTOPE FUEL DEVELOPMENT 15

$^{90}SrF_2$ Compatibility 15
Haynes Alloy No. 25 15
Hastelloy C-276 15
TZM 15

TERRESTRIAL RADIOISOTOPE APPLICATION DEVELOPMENT 17

Cesium-137 Low Solubility Compounds 17
Krypton-85 Light Source Development 20

BENEFICIAL APPLICATIONS OF RADIATION TECHNOLOGY 21

SOLAR-POLAR MISSION MATERIALS SUPPORT

(Activity AE 15 15 20 0, WPAS 02313)

R. L. Heestand

The purpose of this task is to provide direct materials support on work specific to the General Purpose Heat Source (GPHS) design. The scope of this work includes (1) determining the impact properties and optimum weld parameters for the DOP-26 iridium alloy fuel cladding material, (2) thermal conductivity and emissivity data on cladding and thermal insulation materials, (3) fabrication and characterization of test samples of carbon-bonded carbon-fiber (CBCF) insulation developed by ORNL and Y-12 which may be used for GPHS, and (4) determination of creep properties of the 2219 aluminum alloy housing. Data on the impact properties and welding of iridium are integrated with complementary work reported in the Materials Technology section of this report.

CBCF-3 Insulation Fabrication (J M Robbins)

Two rough machined billets, C-16-1 and C-16-5 were shipped to LASL for impact test No. 2. Also two billets, C-16-9 and C-20-1 have been rough machined and two billets C-18-6 and C-18-7 are available for final machining. These billets will be available for future CBCF testing needs.

Five final machined sleeves from run C-20 are being reworked before shipment to LASL for impacts three and four and the aging test. On original inspection, these parts exceeded specification limits on length from six to nine mils. These parts were machined by Continental Machine Co. Inspection of two parts machined by GE and two parts machined by LASL also showed excessive length when inspected by the ORNL Gauge Laboratory.

The consistent over length measurements and some variations in ID and OD measurements when inspected at different locations, further indicate the need for a standard inspection procedure. To qualify machinists and provide sleeves for further inspection, five sleeve blanks were submitted to The Thermo Electron Corp. in Woburn, Massachusetts and five blanks were submitted to Eagle Picher Industries in Oak Ridge, Tennessee.

Minor modification of the dewatering cycle and the rate of heating parts to carbonization temperature are being evaluated as a means of reducing the number of parts that crack during carbonization. The vacuum pump used for the vacuum molding of CBCF has been replaced with a pump capable of the same pumping rate as the Y-12 system. The larger pump capacity should reduce the water to solids ratio of the as-molding material and reduce the variation in density observed in the carbonized material.

CBCF-3 Characterization (G. C. Wei)

Thermal conductivities of specimens from 18 CBCF-3 tubes and three CBCF-3 plates processed at ORNL and carbonized at 1600°C for 3 h and outgassed (1500°C/36 h/5.0E5 torr) were measured by TPRL (Thermophysical Properties Research Lab) of Purdue University. These specimens have densities ranging from 0.201 to 0.245 E3 kg/m^3. Results of the thermal conductivity measurements are shown in Table 1. Least square deviation fit of all the available data points yielded the following relation for thermal conductivity in vacuum as a function of temperature and density,

$$k = -0.06988 + 7.543E\text{-}5 \times T - 1.200E\text{-}11 \times T^3$$

$$+ [0.4364 + 2.128E\text{-}4 \times T + 4.000\text{-}11 \times T^3]\rho,$$

where k is thermal conductivity in vacuum (W/m·K), T is temperature (Kelvin), and ρ is density (E3 kg/m^3). Statistical analysis of the room-temperature data indicated that, at 90% confidence level, a density variation from 0.19 to 0.23 E3 kg/m^3 yielded a thermal conductivity variation from 0.3744 to 0.07181 W/m·K.

Spark source mass spectroscopic analyses of outgassed samples from CBCF-3 tubes C-6-5, C-15-7, and plate P-C-2 showed concentrations of all elements within the specification limit. The results of ash analyses of outgassed samples from CBCF-3 tubes C-6-2, C-6-4, C-6-6, C-16-1, C-16-5, C-16-9, C-18-6, C-18-7, C-20-1, C-20-2, C-20-3, C-20-4, C-20-6, C-20-8, and CBCF-3 plates, P-3-1 and P-3-2 indicated the ash contents all less than 0.3% as required in MRC's specification.

The bulk densities of ORNL-processed CBCF-3 tubes and plates were determined. The results are shown in Table 2. The densities of tubes C-18s, C-19s, C-20s, C-21s, C-22s, C-23s, C-24s, and plates P-2, P-5 were higher than the present specification (0.18 to 0.22 E3 kg/m^3). The cause of the density deviations probably is related to improper determination of carbon fibers used in the molding process.

The compressive strengths of outgassed test samples from tubes C-6s, C-15s, C-16s, C-18s, C-20s, and plates P-3s were measured to be within the specification (>0.52 MPa).

The outgassing furnace used in this program was rebuilt with new furnace heating element and heat shields in this period.

Post-vibration CBCF-3 sleeve C-6-5 was examined. The important conclusions were: (1) no infiltration of particles from FWPF 3D C-C into CBCF-3 was observed; and (2) the powder, collected from the LMRF GPHS module after vibration, consisted of loosened fibers from CBCF-3 parts (about 75%) and particles or fibers from FWPF 3D C-C parts (about 25%).

Table 1. Thermal Conductivity of Outgassed ORNL-Processed CBCF-3 in Vacuum

Part No.	Density ρ (Kg/m^3)	Temperature T(°C)	Thermal Conductivity k(W/m·K)
C-6-5	0.214	23	0.0718
C-6-2	0.209	23	0.0629
C-6-4	0.208	23	0.0611
C-6-6	0.221	23	0.0739
C-15-2	0.222	23	0.0577
C-15-4	0.214	23	0.0482
C-15-7	0.216	23	0.0547
C-16-1	0.207	23	0.0594
C-16-5	0.211	23	0.0563
C-16-9	0.201	23	0.0570
C-18-6	0.243	23	0.0863
C-18-7	0.240	23	0.0788
C-20-1	0.238	23	0.0683
C-20-2	0.231	23	0.0678
C-20-3	0.229	23	0.0688
C-20-4	0.237	23	0.0712
C-20-6	0.228	23	0.0625
C-20-8	0.236	23	0.0693
P-C-2	0.215	23	0.0442
P-3-1	0.239	23	0.0671
P-3-1	0.245	23	0.0720
C-16-5	0.211	800	0.159
C-16-9	0.201	800	0.148
C-16-5	0.211	1400	0.194
C-16-9	0.201	1400	0.189
C-6-5	0.214	1400	0.314
C-6-2	0.209	2000	0.266
C-6-4	0.208	2000	0.255
C-6-6	0.221	2000	0.285
C-15-2	0.222	2000	0.272
C-15-4	0.214	2000	0.226
C-15-7	0.216	2000	0.256
C-16-1	0.207	2000	0.250
C-16-5	0.211	2000	0.241
C-16-9	0.201	2000	0.247
C-18-6	0.243	2000	0.335
C-18-7	0.240	2000	0.336
C-20-1	0.238	2000	0.287
C-20-2	0.231	2000	0.278
C-20-3	0.229	2000	0.266
C-20-4	0.237	2000	0.286
C-20-6	0.228	2000	0.261
C-20-8	0.236	2000	0.264
P-C-2	0.215	2000	0.227
P-3-1	0.239	2000	0.289
P-3-2	0.245	2000	0.280

Table 2. Density of ORNL-fabricated CBCF-3 parts

Part No.	Density (Kg/m^3)			
	Test Samples	Avg. of Test Samples	Pre-Machined Billet	Final Machined Part
C-1-1	--	--	0.224	--
C-2-1	--	--	0.214	--
C-6-1	--	--	0.201	--
C-6-2	0.219 0.214 0.216 0.221	0.218	0.225	--
C-6-4	0.215 0.215 0.214 0.218	0.216	0.222	--
C-6-5	0.213 0.222	0.218	0.222	--
C-6-6	0.220 0.224 0.227 0.219	0.223	0.224	--
C-7-1	--	--	0.209	--
C-8-7	--	--	0.217	--
C-8-8	--	--	0.218	--
C-8-1	0.223 0.216 0.221 0.226	0.222	--	--
C-8-2	0.214 0.209 0.218 0.212	0.213	--	--

Table 2. (Continued)

Part No.	Density (Kg/m^3) Test Samples	Avg. of Test Samples	Pre-Machined Billet	Final Machined Part
C-8-3	0.216 0.223 0.217 0.216	0.218	--	--
C-8-4	0.215 0.213 0.220 0.223	0.214	--	--
C-8-5	0.207 0.217 0.220 0.210	0.214	--	--
C-8-6	0.219 0.222 0.219 0.215	0.219	--	--
C-9-5	--	--	0.206	--
C-9-9	--	--	0.204	--
C-10-8	--	--	0.215	--
C-10-9	--	--	0.213	--
C-15-2	0.219-0.230	0.225	0.222	--
C-15-4	0.216-0.223	0.220	0.222	--
C-15-7	0.219-0.222	0.221	0.221	--
C-16-1	0.207-0.220	0.214	--	--
C-16-5	0.211-0.220	0.216	--	--
C-16-9	0.208-0.215	0.212	--	--

Table 2. (Continued)

Part No.	Density (Kg/m^3)			
	Test Samples	Avg. of Test Samples	Pre-Machined Billet	Final Machined Part
C-18-6	0.241-0.247	0.244	--	--
C-18-7	0.235-0.250	0.238	--	--
C-19	--	--	0.247	--
C-20-1	0.234-0.240	0.237	--	--
C-20-2	0.229-0.236	0.233	--	0.240
C-20-3	0.230-0.238	0.234	--	0.237
C-20-4	0.233-0.244	0.239	--	0.238
C-20-6	0.233-0.236	0.235	--	0.239
C-20-8	0.228-0.237	0.233	--	0.241
C-21	--	--	0.247	--
C-22	--	--	0.258	--
C-23	--	--	0.260	--
C-24	--	--	0.245 0.248	--
P-C-2	0.210-0.218	0.214	--	--
P-2	--	--	0.275	--
P-3-1	0.237-0.260	0.249	--	--
P-3-2	0.238-0.251	0.245	--	--
P-5	--	--	0.263	--

FLIGHT SYSTEMS HARDWARE

(Activity AE 15 20 00 0, WPAS 01322)

D. E. Harasyn

The objective of this task is to supply Mound Facility with flight quality hardware components for use in the assembly of isotope heat sources. The major activity is on fabrication of iridium alloy forming blanks for isotope fuel capsules along with iridium foil for vents, decontamination covers, and weld shields. We have completed fabrication of iridium for the Galileo mission MHW heat source and have initiated fabrication of 1255 iridium blanks and associated foil for Solar-Polar Mission General Purpose Heat Source for delivery in FY 1980 and FY 1981. A new task on fabrication of carbon-bonded carbon-fiber (CBCF) thermal insulation for Light Weight Radioisotope Heating Units (LWRHU) has been deleted due to selection of pyrolytic graphite for the application.

Iridium Blank Fabrication (D. E. Harasyn)

Twenty-eight forming blanks from rework of LR blanks were shipped to MRC in the month of August. Production of blanks from batch powder was delayed because it was noted in the breakdown of the first M ingots that rolling characteristics differed from previous batches. The first indication was cracking of cover plates during initial ingot breakdown and the appearance of surface cracks. Impact ductility tests from the first M sheets gave elongation of approximately 5% when tested under reference impact conditions. Other material properties such as powder chemistry, sheet chemistry, grain size, and hardness all appear normal. Samples of L material impact tested simultaneously showed normal ductility. As the M batch represents the inventory of material intended for completion of FY 1980 deliveries, a contingency plan was developed to continue delivery of discs to MRC. Work initiated immediately on an accelerated schedule consisted of rework of L batch defective blanks and recycle of L batch. In addition, efforts were started to obtain additional iridium powder at the earliest possible date.

As a parallel effort, work on the M batch was continued to obtain the earliest possible impact test on the second batch of ingots. This effort was conducted utilizing overtime in order not to interfere with production.

In addition, an independent ORNL assessment team was assembled to review all production records and procedures used for M batch to identify factors leading to reduced ductility and make recommendations to alleviate the problem.

Due to problems involved with the M batch and the high rejection rate of rolled plates at Mound Facility, a decision was made to roll all subsequent sheet to 0.030 in. (0.76 mm) and grind to final thickness in order to minimize surface defects. Tooling has been developed and put into use to flatten blanks cut from bare rolled sheet for more efficient grinding.

Meetings

R. H. Cooper and A. C. Schaffhauser presented a review of FY 1980 Budget Status and FY 1981 Funding Plans at DOE, Germantown on August 19, 1980.

Creep Properties of 2219 Aluminum Housing Materials (J. P. Hammond)

The purpose of this task is to develop creep design curves on the 2219-T6 aluminum forging and to aid GE, Valley Forge, in the design of the shell component of the RTG generator.

Creep tests are underway with no data to report during this period.

MATERIALS TECHNOLOGY SUPPORT

(Activity AE 15 35 00 0, WPAS 01495)

C. T. Liu

The primary objective of this task is to characterize and improve the metallurgical and mechanical properties of noble base alloys, mainly DOP-26 (Ir-0.3% W doped with 60 ppm Th and 50 ppm Al), to meet the requirements of cladding material in radioisotope heat resources for the Galileo and Solar-Polar space missions. The current efforts are concentrated on four areas: (1) to characterize the impact properties of Ir alloys in the temperature range 800–1400°C, (2) to improve the low-temperature impact properties of welds in the DOP-26 alloy, (3) to identify the mechanism and sources that degrade the mechanical and metallurgical properties of doped Ir alloys under heat-source environments, and (4) to develop ductile high-temperature alloys acceptable for future flight missions.

Impact Properties of M-Batch DOP-26 Alloy (C. T. Liu)

Impact properties of DOP-26 alloy prepared from new M-batch Ir powder were evaluated for flight systems hardware. The impact specimens prepared from different M lots were annealed 19 h at 1500°C and then impacted at 980°C and 61 m/s (200 fps). The impact data on M lots are summarized in Table 3 together with those on L lots. The comparison clearly indicates that the impact ductility of M lots is distinctively lower than that of L lots when impacted at the GPHS conditions. Among the M lots, M-401 prepared from 100% virgin material (WM-1) had the lowest ductility; while M-411 prepared from 42% virgin material (40% WM-8 and 2% WM-3) and 58% head and skull of the ingot M-408 (belong to the M-402 ingot family) had the best ductility. The reason for causing the lower impact ductility of M lots is not known at present time. An internal committee has been established at ORNL to investigate microstructure, grain size, impurity, and grain-boundary chemistry of the M batch powder and production lots.

Sulfur Embrittlement of DOP-26 Alloy (H. Inouye)

The impact ductility of DOP-26 after exposure to $S_2(g)$ are summarized in Table 4. The data confirm that sulfur embrittles the alloy. For a given heat treatment, the extent of embrittlement is greater at 980°C than at 1350°C. The results also suggest that vacuum heat treatments remove most but not all the doped sulfur.

Effect of Phosphorus Contamination on Impact Properties of DOP-26 Alloy (C. T. Liu)

We have previously reported the impact properties of P-doped DOP-26 alloy tested at the MHW conditions, i.e. 1350°C and 85 m/s. According to

Table 3. Tensile Impact Data on M-Batch DOP-26 Production Sheets[a]
Tested at 980°C and 61 m/s

Sheet Number	Impact Elongation (%)	Average Impact Elongation of Each Sheet (%)	Remarks[b]
M-401	5.1 6.0 4.5 4.6	5.1	100% VM
M-406	9.6 9.1 10.1 9.9 6.3	9.0	41% VM and 59% H & S
M-411	13.6 11.5	12.6	42% VM and 58% H & S
M-415	10.8 11.5	11.2	100% VM
M-427	8.7	8.7	100% VM
L-lots	$17.5^{+3.5}_{-2.7}$		40% VM and 60% H & S average of 12 tests

[a]Samples were annealed 19 h at 1500°C in vacuum.

[b]VM = virgin material; H & S = Head and Skull.

Table 4. Impact Ductility of DOP-26 Alloy[a] Exposed to $S_2(g)$

Specimen Number	Heat Treatment[b]	Elongation (%)	Reduction of Area (%)
	At 980°C and 61 m/s		
L-267-1	As doped[c]	4.6	7
L-267-3	As doped + 1 h @ 1500°C	4.5	4
L-267-5	As doped + 1 h @ 1500°C	5.4	23
L-267-6	As doped + 3 h @ 1500°C	8.0	25
L-264	Control	17.8	26
	At 1350°C and 61 m/s		
L-267-2	As doped[c]	15.6	55
L-267-4	As doped + 1 h @ 1500°C	31.4	~100
L-Batch	Control	36	95

[a]Annealed 19 h at 1500°C in vacuum.

[b]In vacuum.

[c]4d at 1175°C and P_{S_2} = ~10 torr.

our Auger electron spectroscopic (AES) analysis, the P doping* for 1 h at 1500°C in a graphite crucible containing P_2O_5 results in a large P concentration on the DOP-26 grain boundaries. The as-doped specimens showed a very low impact ductility (3 ~ 6%) and the impact ductility was recovered completely after vacuum-annealed for 1 h at 1500°C. Annealing P-doped specimens in vacuum at 1500°C reduces the level of phosphorus at the grain boundaries.

In order to determine the effect of P contamination on the impact properties of DOP-26 specimens tested at the GPHS conditions, the P-doped specimens were first annealed at 1500°C for various times in vacuum (to control the P level at the grain boundaries) and then impacted at 980°C and 61 m/s. The P concentration at the grain boundaries of the specimens impacted at 980°C has not been determined by Auger, but is estimated based on the Auger results obtained from the specimens impacted at 1350°C. The impact data obtained at 980°C are plotted as a function of the Auger peak height ratio, P (120 eV)/Ir (229 eV), together with those at 1350°C in Fig. 1. DOP-26 appears to be much more sensitive to the level of P contamination at the grain boundaries when impacted at 980°C. The alloy remains brittle until the P/Ir ratio is less than 0.18. In comparison, the alloy can tolerate a P ratio (P/Ir) of 0.45 at the 1350°C impact.

AES Analysis of M-Lot DOP-26 Alloy (C. L. White and R. A. Padgett)

In an effort to determine the cause of the reduced impact ductility of M-lot DOP-26 material tested at 980°C and 61 m/s, AES analysis of specimens from heats M-401 and L-294 (as a control) were performed. Samples 800045-C (M-401-B) and 800047-B (L-294-B) were cut from sheet, adjacent to locations where impact specimens had been punched. These specimens were annealed 19 h at 1500°C in vacuum prior to AES analysis.

Comparison of Auger spectra from fresh intergranular fracture surfaces of these specimens failed to reveal any trace impurities that might be responsible for the reduced impact ductility of the M-lot material. Specifically, no trace of phosphorus or sulfur was observed in 800045-C, and oxygen levels were similar to those observed in 800047-B and other DOP-26 heats exhibiting good impact ductility. The thorium level observed on the fracture surface of 800045-C was also similar to that observed for 800047-B and other "good" DOP-26 heats.

Development of Pt-Base Alloys (J. R. Keiser and J. F. Newsome)

The purpose of this work is to develop new platinum-base alloys suitable for use as fuel-cladding materials for space flight missions. Requirements include an adequately high eutectic temperature with graphite and sufficient impact and tensile strength at 800–850°C after both extended operation at 1260°C and a reentry condition of 2 minutes at 1540°C. On the basis of eutectic studies of alloys with graphite and

*The P doping was performed at LASL. The specimens were annealed for 18 h at 1500°C in vacuum prior to P-doping.

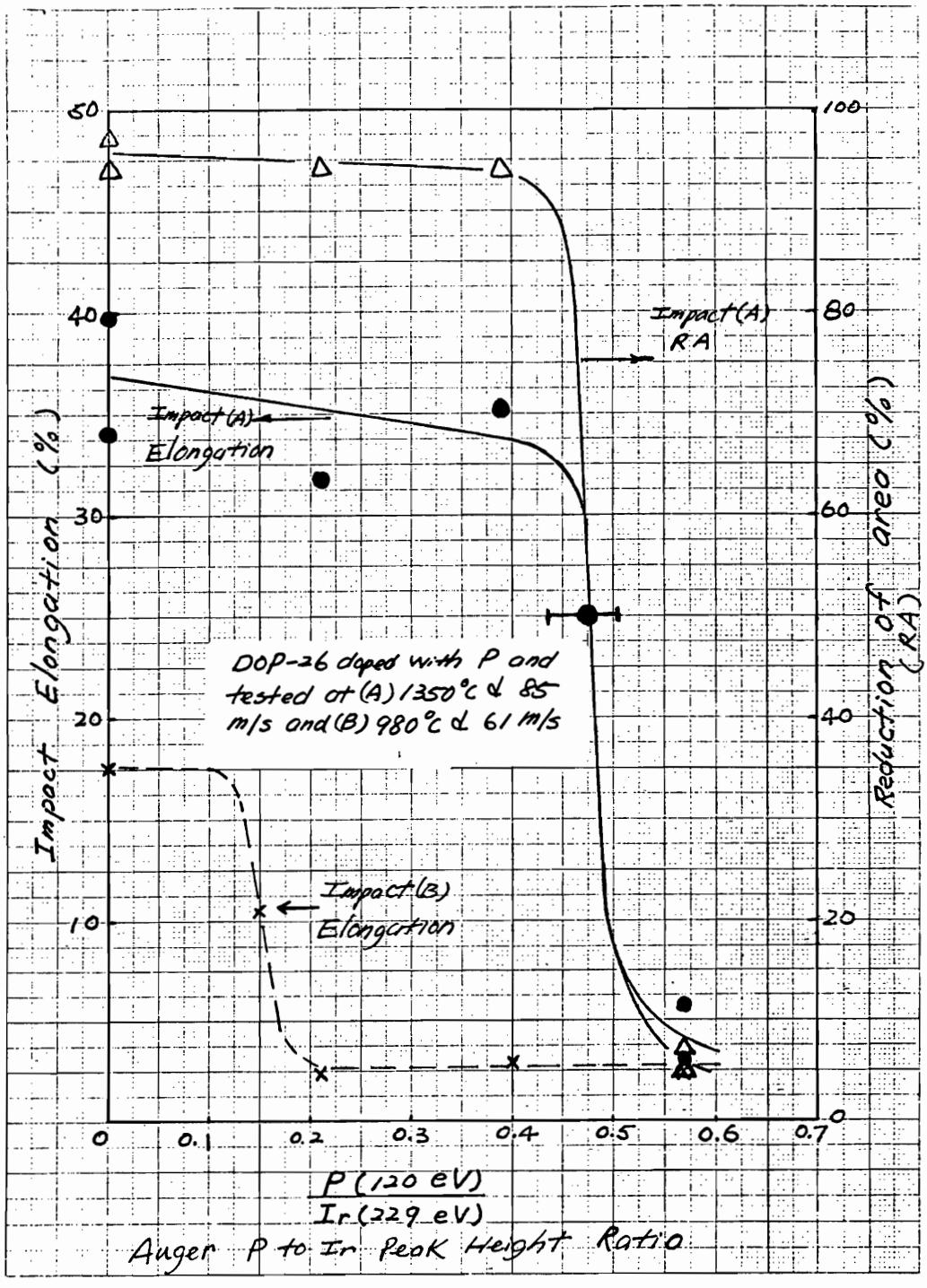

Fig. 1. Plot of impact elongation and reduction of area of P-doped DOP-26 specimens tested at (a) 1350°C and 85 m/s and (b) 980°C and 61 m/ as a function of Auger peak height ratio, P (120 eV)/Ir (229 eV).

impact tests at 800°C, four binary alloys were chosen for further study. (Ternary systems will be studied later). Alloys selected were:

Pt–12 wt % Re
–16 wt % Re
–20 wt % Ru
–30 wt % Ru

Sheets of these four alloys are being fabricated. In order to determine annealing temperatures for these alloys, a brief study is being made in which samples from each of the alloys are held 1 h at 800, 1000, 1100, 1200 or 1300°C. From this study we will be able to recommend an annealing temperature to be used during the final steps of fabrication of the four alloys.

Once we receive the sheet we will determine the slow strain rate tensile strength between room temperature and 1400°C and the impact strength at 61 m/s between 500 and 1000°C.

ISOTOPE FUEL DEVELOPMENT

(Activity AE 15 35 00 0, WPAS 02314)

R. S. Crouse

$^{90}SrF_2$ Compatibility (R. S. Crouse)

Microprobe examination of the 30,000 h test of $^{90}SrF_2$ compatibility tests has been completed and the data sent to H. T. Fullam, Battelle, PNL. Because of the complexity of the test systems, it was felt that the most information could be obtained and displayed by making x-ray dot maps of the elemental distribution in the attack zones. Polaroid photographs of the dot maps along with a text of explanation were sent to Fullam.

A summary of the results follows:

Haynes Alloy No. 25

At 600°C the corrosion zone differs in apparently duplicate samples. In one case, Cr and Fe are reacted leaving a concentration of Ni and Co in the base material. In the other, the corrosion contains all four elements in separate strata with Ni and Co again together and the Cr and Fe together except in one strata where Cr is also concentrated with Ni and Co. Very confusing. In neither sample does Sr seem to participate in the reaction. It does adhere to the surface.

At 800°C all four of the elements in the alloy are found in the corrosion with Cr tending to concentrate next to the unattacked metal. Inexplicably, W appears erratically associated with Cr at some places and the Fe, Ni and Co at others. Once again Sr seems to not be especially involved.

Hastelloy C-276

At 600°C there appears to be partitioning of the alloy elements in the corrosion zone. Iron and Cr tend to be together and separate from the ni rich areas. Strontium does not seem to be much involved. At 800°C a heavy zone of Cr rich corrosion product occured on the surface of the sample. There was also some obvious attack along some dendritic structure over much of the sample. This attack was rich in Cr and Sr and poor in Ni and Fe. Apparently, under these conditions Sr reacted with Cr. It seems likely that this dendritic structure was in the original microstructure, and may have Cr rich from the beginning.

TZM

This alloy was generally resistant to attack in $^{90}SrF_2$. Some effect was seen in relatively narrow zones along the surface in the form of Mo depletion. This seemed to be just a general removal of material along

the striae of the fibrous microstructure. At 800°C there seemed to be some back filling by Sr of the openings produced in this attack. Otherwise, Sr does not seem to be involved.

In summary, it can be said that the microprobe examination begins to shed a little light on the mechanisms of the attack in these tests. However, the systems are so complex and the variables so many that we have only begun to scratch the surface in understanding what is going on. It was not the purpose of these tests to answer the myriad of questions one might ask about rates and mechanisms. It is beyond what was done.

This report concludes this program. The data has all been transmitted to Fullam at Battelle PNL and this highlight wraps it up.

TERRESTRIAL RADIOISOTOPE APPLICATION DEVELOPMENT

(Activity AE 15 35 00 0, WPAS 01367)

F. N. Case, K. W. Haff, and F. J. Schultz

Cesium-137 Low Solubility Compounds

Leaching of the unsectioned, fully loaded ^{137}Cs aluminosilicate pellets continued this month. The leach rates are given below in Table 5.

Table 5. Unsectioned, Fully Loaded Cesium-137 Aluminosilicate Pellet Leach Rates

Sample No.	Leaching Period Interval (days)	Accumulated Leaching Period (days)	Leach Rate ($kg\ m^{-2} \cdot s^{-1}$)
1-9	0.784	3.940	8.220×10^{-12}
1-10	0.270	4.210	9.946×10^{-12}
1-11	2.719	6.929	3.406×10^{-12}
1-12	1.000	7.929	1.816×10^{-12}
1-13	1.033	8.962	3.103×10^{-12}
1-14	0.969	9.931	2.922×10^{-12}
1-15	0.994	10.925	3.273×10^{-12}
1-16	3.043	13.968	2.187×10^{-12}
2-9	0.788	3.935	1.912×10^{-11}
2-10	0.267	4.202	2.597×10^{-11}
2-11/25	2.763	6.965	9.904×10^{-12}
2-12	0.958	7.923	1.204×10^{-12}
2-13	1.031	8.954	7.086×10^{-12}
2-14	0.972	9.926	4.291×10^{-12}
2-15	0.950	10.876	5.171×10^{-12}
2-16	3.052	13.928	6.535×10^{-12}

The static experiment leach rates have decreased by a factor of approximately 2 since the last reporting period. However, the leach rates are decreasing less rapidly and appear to be approaching steady-state values.

Leaching of the sectioned, fully loaded ^{137}Cs aluminosilicate pellets in the Soxhlet extractors continued this month. The leach rates of each pellet are presented in Table 6.

The leach rates are still decreasing and, therefore, have not attained steady-state values.

Table 6. Leach Rates of Fully Loaded Cesium-137 Aluminosilicate Pellets

Sample No.	Leaching Period Interval (days)	Accumulated Leaching Period (days)	Leach Rate ($kg\ m^{-2} \cdot s^{-1}$)
5-7/25	7.911	27.495	1.80×10^{-11}
5-8/25	5.898	33.393	1.35×10^{-10}
5-9/25	6.932	40.325	1.54×10^{-8}
5-10/25	6.901	47.226	4.18×10^{-9}
6-7/25	7.911	27.495	2.65×10^{-9}
6-8/25	5.898	33.393	*
6-9/25	6.932	40.325	3.66×10^{-9}
6-10/25	6.901	47.226	3.15×10^{-9}
7-7/25	7.911	27.495	1.02×10^{-9}
7-8/25	5.898	33.393	1.38×10^{-9}
7-9/25	6.932	40.325	1.07×10^{-9}
7-10/25	6.901	47.226	5.64×10^{-10}
8-7/25	7.911	27.495	3.30×10^{-9}
8-8/25	5.898	33.393	3.48×10^{-9}
8-9/25	6.932	40.325	2.99×10^{-9}
8-10/25	6.901	47.226	3.23×10^{-9}

*Sample 6-8/25 spilled during collection.

Leaching of the irradiated tracer-level ^{137}Cs aluminosilicate pellets was begun this month. The leach rates are reported in Table 7.

Table 7. Leach Rates of Irradiated Tracer-Level Cesium-137 Aluminosilicate Pellets

Sample No.	Leaching Period Interval (days)	Accumulated Leaching Period (days)	Leach Rate ($kg\ m^{-2} \cdot s^{-1}$)
Sox 1-IRR-1A	0.980	0.980	4.05×10^{-8}
Sox 1-IRR-2	0.953	1.933	3.63×10^{-8}
Sox 1-IRR-3	1.008	2.941	3.77×10^{-8}
Sox 1-IRR-4	0.950	3.891	3.24×10^{-8}
Sox 1-IRR-5	3.024	6.915	3.19×10^{-8}
Sox 1-IRR-6	2.978	9.713	3.07×10^{-8}
Sox 1-IRR-7	4.979	14.692	2.74×10^{-8}
Sox 2-IRR-1A	0.980	0.980	1.28×10^{-8}
Sox 2-IRR-2	0.953	1.933	1.36×10^{-8}
Sox 3-IRR-3	1.008	2.941	1.41×10^{-8}
Sox 2-IRR-4	0.950	3.891	1.50×10^{-8}
Sox 2-IRR-5	3.024	6.915	1.17×10^{-8}
Sox 2-IRR-6	2.978	9.713	1.09×10^{-8}
Sox 2-IRR-7	4.979	14.692	3.13×10^{-9}*
Sox 3-IRR-1A	0.980	0.980	2.24×10^{-8}
Sox 3-IRR-2	0.953	1.923	3.08×10^{-8}
Sox 3-IRR-3	1.008	2.941	3.19×10^{-8}
Sox 3-IRR-4	0.950	3.891	3.28×10^{-8}
Sox 3-IRR-5	3.024	6.915	2.47×10^{-8}
Sox 3-IRR-6	2.978	9.713	2.63×10^{-8}
Sox 3-IRR-7	4.979	14.692	2.32×10^{-8}

*The sample volume collected was reduced due to a malfunctioning condenser tube and, consequently, some entrained cesium atoms were lost with the escaping vapors.

A comparison of the leach rates of the tracer level ^{137}Cs aluminosilicate pellets before and after irradiation in a high energy gamma-ray field is shown in Table 8.

Table 8. Leach Rates of Pre-Irradiated and Irradiated Tracer Level Cesium-137 Aluminosilicate Pellets

Sample No.	Accumulated Leaching Period (days)	Leach Rate ($kg\ m^{-2} \cdot s^{-1}$)
Sox 1-8832	368	2.65×10^{-8}
Sox 2-8832	368	1.02×10^{-8}
Sox 3-8832	368	2.34×10^{-8}
Sox 1-IRR-7	15	2.74×10^{-8}
Sox 2-IRR-6	10	1.09×10^{-8}
Sox 3-IRR-7	15	2.32×10^{-8}

The comparison reveals no difference (within experimental error) between the leach rates of the pre-irradiated and irradiated pellets. This suggests that the high energy gamma-ray field had little or no effect on the cesium leachability of the cesium aluminosilicate pellets.

Krypton-85 Light Source Development

Discussions were held with instrument and control personnel concerning optics systems that might provide alternatives to the light pipe concept now used for ^{85}Kr lights. While the advantages of reflector-type light transmission in altering the direction of light emission is apparent, shielding problems make light pipe configuration attractive.

A quartz bulb type geometry was designed and placed in fabrication. Special radiation resistant quartz will be used and it will be treated with hydrofluoric acid to remove microscopic surface stress points to provide maximum mechanical strength. This geometry may permit better light collection when compared with the quartz helix geometry.

A meeting was scheduled with DOE, DOD, and ORNL personnel to firm up the requirements all participants will have for the FY 1981 effort and to agree upon the technical advisory committee makeup and to discuss the DOD reporting format required to meet their work scope specifications.

BENEFICIAL APPLICATIONS OF RADIATION TECHNOLOGY

(Activity AE 15 35 00 0, WPAS BART001)

C. S. Sims

The document entitled *Assessment of the* ^{137}*Cs Irradiation Technology Program*, ORNL/CF-80/262, was distributed during the last week of August.

Oak Ridge National Laboratory personnel made preliminary operational radiation dose measurements at the Sandia Irradiator for Dried Sewage Solids on August 22. Further measurements are planned for the second week in September.

Preliminary laboratory scale irradiations of microbiological samples (e.g., Escherichia coli) using approximately 17kCi of ^{60}Co were performed on August 12 and August 20. These experiments were the first radiation experiments performed by the program team and were designed to verify expected radiation sensitivities. Doses of approximately 100, 200, and 300 krad (H_2O) were used.

INTERNAL DISTRIBUTION

1. E. E. Bloom
2. C. R. Brinkman
3. J. A. Carter
4. F. N. Case
5–10. R. H. Cooper
11. R. S. Crouse
12. J. E. Cunningham
13. S. A. David
14. J. H. DeVan
15. R. G. Donnelly
16. W. P. Eatherly
17. J. I. Federer
18. G. M. Goodwin
19. K. W. Haff
20. J. P. Hammond
21. W. O. Harms
22. R. L. Heestand
23. M. R. Hill
24. J. R. Keiser
25. J. W. Koger
26. H. Inouye
27. E. Lamb
28. C. T. Liu
29. D. L. McElroy
30. C. D. Montgomery
31. T. K. Roche
32. A. C. Schaffhauser
33. C. S. Sims
34. G. M. Slaughter
35. J. O. Stiegler
36. V. J. Tennery
37. D. B. Trauger
38. G. C. Wei
39. J. R. Weir, Jr.
40. C. L. White
41–45. Laboratory Records
46. Laboratory Records, ORNL RC
47. ORNL Patent Office

EXTERNAL DISTRIBUTION

48–59. DOE Space and Terrestrial Systems Division, Washington, DC 20545

G. L. Bennett
R. C. Brouns
F. M. Dieringer
N. Goldenberg
J. S. Griffo
W. D. Kenney
J. J. Lombardo
R. B. Morrow
P. A. O'Riordan
W. C. Remini
B. J. Rock
C. O. Tarr

60–61. DOE Albuquerque Operations Office, P.O. Box 5400, Albuquerque, NM 87115

D. K. Nowlin
D. Plymale

62–63. DOE Oak Ridge Operations Office, P.O. Box E, Oak Ridge, TN 37830

J. A. Lenhard
J. Pidkowicz

64–65. DOE San Francisco Operations Office, 1333 Broadway, Wells Fargo Building, Oakland, CA 94612

L. Lanni
W. L. Von Flue

66–67. DOE Savannah River Operations Office, P.O. Box A, Aiken, SC 29801

W. T. Goldston
W. D. Sandberg

68. DOE Dayton Area Office, P.O. Box 66, Miamisburg, OH 45342

H. N. Hill

69. Air Force Weapons Laboratory, Kirtland Air Force Base, DYUS, Albuquerque, NM 87116

Michael Seaton

70–71. Battelle Columbus Laboratories, 505 King Ave., Columbus, OH 43201

E. L. Foster
I. M. Grinberg

72–73. E. I. du Pont de Nemours, Savannah River Plant, Aiken, SC 29801

R. A. Brownback
W. R. Kanne

74–75. E. I. du Pont de Nemours, Savannah River Laboratory, Aiken, SC 29801

R. L. Folger
R. H. Tait

76–77. Fairchild Industries, 20301 Century Blvd., Germantown, MD 20767

M. Eck
A. Schock

78. General Atomic Co., P.O. Box 81608, San Diego, CA 92138

N. B. Elsner

79–81. General Electric Co., Valley Forge Space Center, P.O. Box 8048, Philadelphia, PA 19101

V. Haley
R. J. Hemler
C. W. Whitmore

82–84. Jet Propulsion Laboratory, California Institute of Technology, 4800 Oak Grove Drive, Pasadena, CA 91103

R. W. Campbell
J. E. Mondt
A. E. Wolfe

85. Johns Hopkins University, Applied Physics Laboratory, Johns Hopkins Road, Laurel, MD 20810

J. C. Hagan

86–88. Los Alamos National Scientific Laboratory, P.O. Box 1663, Los Alamos, NM 87545

S. E. Bronisz
S. S. Hecker
W. J. Maraman

89–91. Minnesota Mining and Manufacturing Co., St. Paul, MN 55101

R. B. Ericson
J. D. Hinderman
W. C. Mitchell

92–93. Monsanto Research Corp., P.O. Box 32, Miamisburg, OH 45342

E. W. Johnson
W. C. Wyder

94. Sundstrand Energy Systems, 4747 Harrison Ave., Rockford, IL 61101

E. Krueger

95–96. Teledyne Energy Systems, 110 W. Timonium Rd., Timonium, MD 21093

W. J. Barnett
W. E. Osmeyer